Engineering Science and Technology, an International Journal xxx (2016) xxx–xxx

HOSTED BY

ELSEVIER

Contents lists available at ScienceDirect

Engineering Science and Technology, an International Journal

journal homepage: www.elsevier.com/locate/jestch

Full Length Article

Compact printed high rejection triple band-notch UWB antenna with multiple wireless applications

Manish Sharma [a], Y.K. Awasthi [b,*], Himanshu Singh [c], Raj Kumar [d], Sarita Kumari [e]

[a] Department of Electronics Engineering, Banasthali University, Rajasthan & Aravali College of Engineering and Management, Faridabad, India
[b] Department of Electronics & Communication Engineering, Antenna Fabrication & Measurement Laboratory, Manav Rachna University, Faridabad, Haryana 121003, India
[c] Department of Electronic Science, Sri Aurobindo College, (University of Delhi) Malviya Nagar, New Delhi 110017, India
[d] Department of Electronics & Communication Engineering, M R K Institute of Engineering & Technology, Rewari, Haryana 123401, India
[e] University of Rajasthan, Jaipur, Rajasthan 302004, India

ARTICLE INFO

Article history:
Received 12 April 2016
Revised 20 May 2016
Accepted 20 May 2016
Available online xxxx

Keywords:
Urn shape
Multiple wireless services
T-shape stub
WLAN
WiMAX

ABSTRACT

In this paper, small printed urn-shape triple notch ultra-wideband (UWB) monopole antenna with diverse wireless applications is presented. Notch bands include WiMAX (IEEE802.16 3.30–3.80 GHz), WLAN IEEE802.11a/h/j/n (5.15–5.35 GHz, 5.25–5.35 GHz, 5.47–5.725 GHz, 5.725–5.825 GHz), and X-band downlink satellite system (7.25–7.75 GHz) and other multiple wireless services as close range radar (8–12 GHz) in X-band & satellite communication (12–18 GHz) in Ku-band. By including T-shape stub and etching two C-shaped slots on the radiating patch, triple band-notch function is obtained with measured high band rejection (VSWR = 16.54 at 3.60 GHz, VSWR = 22.35 at 5.64 GHz and VSWR = 6.38 at 7.64 GHz) and covers a wide useable fractional bandwidth of 154.56% (2.49–19.41 GHz). In short the antenna offers triple band-notch UWB systems as a compact multifunctional antenna to reduce the number of antennas installed in wireless devices for accessing multiple wireless networks with wide radiation pattern.
© 2016 The Authors. Publishing services by Elsevier B.V. on behalf of Karabuk University. This is an open access article under the CC BY-NC-ND license (http://creativecommons.org/licenses/by-nc-nd/4.0/).

1. Introduction

Since the Federal Communication Commission (FCC) introduced the unlicensed ultra wideband (UWB) from 3.1 to 10.6 GHz with 109.5% fractional bandwidth for commercial communication applications, many types of UWB antenna have been reported. Additional extra frequency band at 2.4 GHz (Bluetooth band) and two frequency notch-bands (WiMAX/WLAN) are created by inserting the stubs of quarter-wavelength to the ground plane near the feed line. The impedance bandwidth is increased by beveling lower edge of the slot near the feed line by an angle α [1]. A T-shaped stub in the radiating patch and two U-shaped stubs beside the feed line are realized to obtain dual-band-notch characteristics. Impedance bandwidth is tuned by optimizing the gap between radiation patch and ground plane. The beveled ground plane provides smooth transition from one resonance mode to another ensuring good impedance bandwidth and stable gain [2]. Additional resonance is excited and bandwidth is improved by cutting an inverted Fork-shaped slit on the ground plane. The notch for the desired bands is achieved by electromagnetically coupling between coupled inverted U-ring strip and cross-shaped radiating patch. By cutting an inverted T-shaped slot impedance bandwidth at high frequency is obtained [3]. Moreover, C-shaped slot surrounding T-shaped slot and adding an inverted T-shaped parasitic structure inside the inverted T-shaped slot on the radiating patch yields dual band-notched function [4]. As reported, a T-shaped slot in the radiating patch provides strong notch band rejections up to VSWR = 26 which is tunable over a wide frequency range from 3.55 GHz to 6.80 GHz [5]. A microstrip-line feed beak-shaped monopole-like slot UWB antenna finds its applications in UWB, Bluetooth, GSM and GPS wireless communication systems. Two rectangular slot in the beak-shaped radiator and the hexagonal-shaped DGS are used to obtain GPS (1.520–1.590 GHz), GSM (1.770–1.840 GHz) and Bluetooth (92.385–2.490 GHz). Furthermore, bandwidth of the antenna is enhanced by etching a triangular slot at the junction of patch and feed line [6]. As reported in [7], multi-band planar monopole is obtained firstly by etching center portion of the radiating patch which is diamond-like shape and secondly by inserting quarter wavelength slits on the central part of radiating patch. Quarter wavelength slits corresponds to frequency bands of 1.3 GHz (GPS), 1.8 GHz (GSM), 2.4 GHz (Lower band WLAN) and diamond-shape radiating patch corresponds to UWB band

* Corresponding author.
E-mail addresses: manishengineer1978@gmail.com (M. Sharma), yogendra@mru.edu.in (Y.K. Awasthi), kajal_172@rediffmail.com (H. Singh), raj_indya2000@yahoo.com (R. Kumar), sarita.kumari132@gmail.com (S. Kumari).

Peer review under responsibility of Karabuk University.

http://dx.doi.org/10.1016/j.jestch.2016.05.011
2215-0986/© 2016 The Authors. Publishing services by Elsevier B.V. on behalf of Karabuk University.
This is an open access article under the CC BY-NC-ND license (http://creativecommons.org/licenses/by-nc-nd/4.0/).

Please cite this article in press as: M. Sharma et al., Compact printed high rejection triple band-notch UWB antenna with multiple wireless applications, Eng. Sci. Tech., Int. J. (2016), http://dx.doi.org/10.1016/j.jestch.2016.05.011

(3.10–10.60 GHz). In [8], monopole antenna which operates in dual band (WLAN/UWB) is reported for Multi-Input–Multi-Output/Diversity applications consisting U-shaped patch along with T-shaped monopole path and pentagonal wide slot ground plane. The metallic surfaces of microstrip antennas cause a large RCS values. But RCS reduction in the ultra-wideband range is difficult. So an Octagonal-shaped antenna with reduced Radar Cross Section (RCS) is reported to cover extended UWB (2.5–18.0 GHz) with 151% fractional bandwidth [9]. However, promising mechanical and thermal properties of thermoplastic acrylonitrile butadiene styrene polycarbonate (ABC-PC) substrate has been reported for integration in molded interconnects devices technology [10]. Due to reduction in size and symmetric in shape, monopole and quasi-monopole antennas are easily incorporable solutions for portable devices [11]. Therefore, Vivaldi antenna with the dimensions of $42 \times 36 \times 1.6\ mm^3$ is reported. Structural modification in the radiating fins has increased the electrical length thereby reducing the lower operating frequency from 5.2 GHz to 3.7 GHz and antenna maintains −20 dB co-polarization to cross-polarization ratio throughout the bandwidth [12]. A switchable monopole antenna in UWB band and dual-band mode is triggered by LED. In the switch-OFF mode, antenna operates in UWB band while in switch-ON state the configuration converts to dual-band antenna due to extended ground plane [13]. A single notch UWB antenna is reported in [14] which consist of fractal patch with an array of fractal unit cells oriented to resemble the branches of tree. To obtain WiMAX (IEEE 802.16) and C-band systems, T-shaped stub is embedded on the fractal patch. Electromagnetic coupling theory (ECT) can create band-notch function by butterfly-shape parasitic element on backplane of radiating patch and 155% bandwidth enhancement is achieved by rectangular shaped slots on ground plane [15]. A conical shape monopole antenna for UWB applications has been reported with multiple wireless applications including close range radar & satellite communication [16–18]. Fractal Koch along with T-shaped stub results in triple-notch band which are centered at 2 GHz, 3.5 GHz and 5.8 GHz respectively for Personal Communication Systems (PCS), Worldwide Interoperability for Microwave Access (WiMAX) and Wireless Local Area Network (WLAN) is reported in [20]. Reported antenna has maximum gain of 6.5 dBi. Introduction of two arc shaped elliptical slots on the circular ring radiating patch with a pair of rectangular single split ring resonators near the feed line can band notch WiMAX/WLAN/X-band downlink satellite system [21–29]. Furthermore, by incorporating an inverted U-slot and an inverted C-slot etched on radiating patch with a U-slot on the microstrip feed line are responsible for tri-band notch characteristics (3.3–3.8, 5.15–5.825, 7.1–7.9 GHz) [30]. Moreover, tri-notch band characteristics is also obtained on semicircular radiating patch and a modified ground plane with two bevels at upper edge by etching two round shape slots in radiating patch and pair of rotated V-shaped slot in ground plane [31]. Uniform omni-directional patterns and stable linear polarizations can be developed by introducing a ground-cooperative radiating structure (GCRS) into the metal ground of a prototype defected hexagonal monopole antenna (HMA) [32]. Multimode-resonator filter consisting of a single-wing element is combined with the modified slot UWB antenna providing a 6 dB increase in the realized gain near 10 GHz [33]. A CPW fed monopole with spiral slot etched on the patch is reported. Tri-notch bands can be obtained by varying the length of a single spiral slot and dual polarization UWB achieved by slotted monopole antenna [34–35]. Thus, the microstrip UWB antenna designs have promising application values because of its low profile, easy fabrication and low production cost.

The design of UWB antenna with triple notch in low profile has two critical problems. One is to introduce triple band-notches in very small size; the second is to preserve radiation properties of antenna in the whole operation band. To overcome these problems, we present a very small high rejection triple band-notch UWB antenna, reducing the size ($20 \times 20 \times 0.787\ mm^3$) by 55% in comparison with the previously published work as compares in Table 2 and also wider bandwidth for multiple wireless services including close range radar: 8–12 GHz in X-band & satellite communication: 12–18 GHz in Ku-band is obtained (2.49–19.41 GHz) by embedding dual identical ellipse on hexagonal radiating patch. A T-shape stub along with two C-shape slots in the radiating patch is responsible for triple band-notch characteristics. Meanwhile, this antenna exhibits excellent time domain analysis with almost constant group delay of variation less than 1.0 ns. These merits make it qualified as a compact multifunctional antenna to reduce the number of antennas installed in compact wireless devices for wireless applications. The radiation patterns and scattering characteristics are simulated and experimentally verified.

2. Antenna design and analysis

Geometry of proposed antenna with the capability adding rejecting bands is shown in Fig. 1. The proposed antenna is printed on Rogers RT/Duroid 5880 substrate of thickness 0.787 mm with relative permittivity $\varepsilon_r = 2.33$, $\tan\delta = 0.012$. From Fig. 1(a), antenna has compact dimensions of $W_{sub} \times L_{sub} = 20 \times 20\ mm^2$ or about $0.28\lambda \times 0.28\lambda$ at 4.2 GHz (λ corresponds to first resonance frequency at 4.2 GHz) which is fed with 50Ω microstrip line with optimized dimensions of $W_f \times L_f$. The basic antenna structure consisting radiating patch as shown in Fig. 1(b) comprises of basic hexagonal shape, each side of 8 mm merged with two identical ellipses of major radius 9 mm by eccentricity ratio of 0.33 is embedded for wider bandwidth and ground plane dimensions of $W_g \times L_g = 20 \times 5\ mm^2$. Fig. 1(c) represents front view of antenna with triple band-notch function. A T-shape stub is inserted on the radiating patch for WiMAX band and two C-shaped slots for WLAN and X-band downlink satellite system. The parameters of proposed antenna are optimized using ANSYS High Frequency Structural Simulator (HFSS). The length of the first, second and third notches are calculated by using following equations and width of stub and slots is optimized with 0.5 mm. The value of $f_{FirstNotch}$, $f_{SecondNotch}$ and $f_{ThirdNotch}$ are calculated at center notched frequency of 3.56 GHz, 5.58 GHz and 7.47 GHz respectively.

$$L_{NotchBand} = \frac{c}{2 \times f_{CenterFrequency} \sqrt{\varepsilon_{eff}}} \tag{1}$$

$$\varepsilon_{reff} = \frac{\varepsilon_r + 1}{2} + \frac{\varepsilon_r - 1}{2}\left[1 + 12\frac{h_{sub}}{W_f}\right]^{\frac{-1}{2}} \tag{2}$$

where c is speed of EM wave in free space and is given by $c = 3 \times 10^8$ m/s. From Ref. [19], effective relative permittivity of substrate is calculated ε_{reff} (w_f/h_{sub}, ε_r, f). Optimized parameter of the proposed antenna are as follows: $W_{sub} = 20$ mm, $L_{sub} = 20$ mm, $h_{sub} = 0.787$ mm, $MR_1 = 8$ mm, $MR_2 = 5.71$ mm, $W_f = 2$ mm, $L_f = 6.0$ - mm, $W_g = 20$ mm, $L_g = 5$ mm, $S_1 = 12$ mm, $S_2 = 6$ mm, $T_1 = 5$ mm, $T_2 = 11$ mm, $W_1 = 9$ mm, $W_2 = 7$ mm, $W_3 = 3.00$ mm, $W_4 = 2.75$ mm, $L_1 = 4.75$ mm, $L_2 = 3$ mm, $t_1 = 0.5$ mm, $t_2 = 0.5$ mm, $t_3 = 0.5$ mm, $L_p = 10$ mm.

Length of each side of polygon patch is calculated by Eq. (3).

$$L_p = \frac{c}{4 \times f}\sqrt{2/(1 + \varepsilon_{reff})} \tag{3}$$

where f corresponds to first resonance frequency and ε_{reff} is the effective permittivity. Fig. 2 shows the structure of various antennas used for simulation studies and corresponding VSWR is represented in Fig. 3. The proposed antenna with hexagonal shape radiating patch and rectangular ground plane covers partial bandwidth

Please cite this article in press as: M. Sharma et al., Compact printed high rejection triple band-notch UWB antenna with multiple wireless applications, Eng. Sci. Tech., Int. J. (2016), http://dx.doi.org/10.1016/j.jestch.2016.05.011

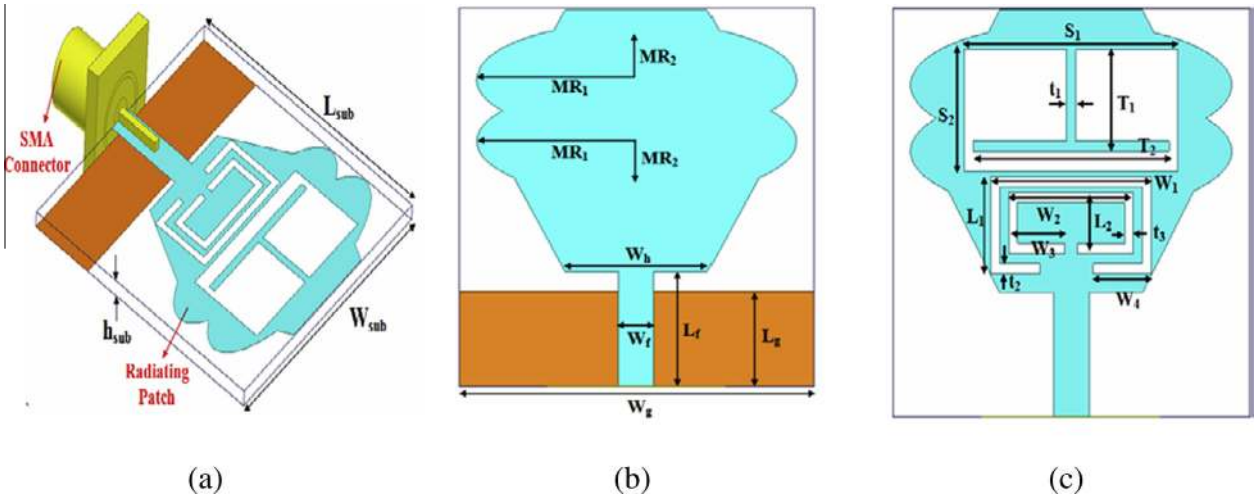

Fig. 1. Geometry of the proposed UWB antenna (a) Slant View. (b) Front view with ground plane. (c) Front view with triple notch.

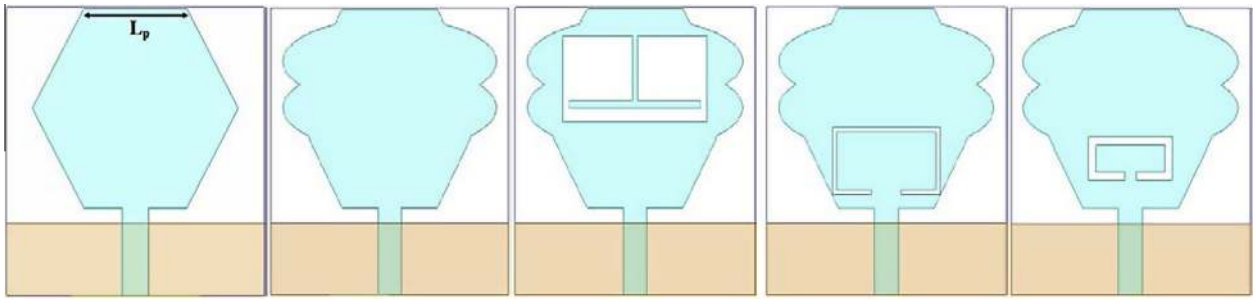

Fig. 2. (a) Monopole antenna with partial UWB bandwidth (b) Basic monopole UWB antenna (c) WiMAX notch (d) WLAN notch (e) X-band downlink satellite system notch.

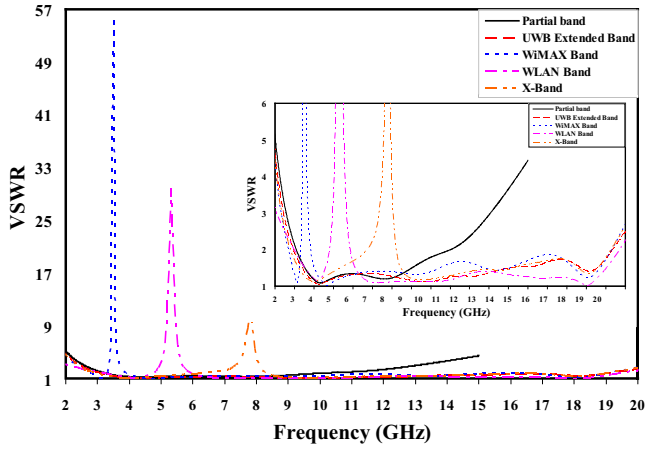

Fig. 3. VSWR comparison from ordinary monopole to proposed antenna.

(2.97–11.14 GHz) which is shown in Fig. 3. As illustrated in Fig. 2(b), dual ellipse is embedded on the hexagonal shape radiating patch which results in extension of impedance bandwidth from 2.42 GHz to 19.12 GHz. As depicted from Fig. 3, antenna exhibits good impedance match for VSWR $\leqslant$ 2 in the entire operating band. A inverted T-shape stub on the radiation patch as shown in Fig. 2(c) results in removal of WiMAX from 3.25 to 3.82 GHz. The WLAN band is eliminated by etching C-shape slot as shown in Fig. 2(d) removing 4.83–5.99 GHz. According to Fig. 2(e), X-band is eliminated confirming the removal of 7.18–7.72 GHz band.

From Fig. 3, simulated proposed antenna shows high band rejection at 3.56 GHz with VSWR = 9.90, 5.58 GHz with VSWR = 32.36 and 7.47 GHz with VSWR = 9.90.

3. Parametric study of high band rejection

The proposed antenna is optimized and investigated by full wave EM solver, Ansoft HFSS. The centre frequency of notch bands along with peak value of VSWRs is controlled by the length of inverted stub and slots, as described below:

3.1. Effect of stub length (T_1)

Fig. 4(a) represents simulated parametric variation of T_1 with constant value of T_2 (11 mm) for WiMAX band. By varying T_1 of T-shaped stub, wide shift of band-notch is observed from 3.17–3.89 GHz to 4.952–5.978 GHz which infers that length T_1 is alone capable of covering both WiMAX and WLAN bands with VSWR varying from 55.81 to 12.87 respectively. The length of T_1 from 2.0 mm to 5.0 mm is varied and shifting of band can be seen from higher to lower frequency side. The length T_1 is tuned to 5 mm with maximum VSWR of 55.81 to achieve intended notch band.

During optimization of T_1, it has been observed that impedance bandwidth is maintained in the entire band (2.49–19.41 GHz) significantly.

3.2. Effect of stub length (T_2)

Fig. 4(b) represents simulated parametric variation of T_2 with constant value of T_1 (5 mm) also for WiMAX band. By varying T_2

Please cite this article in press as: M. Sharma et al., Compact printed high rejection triple band-notch UWB antenna with multiple wireless applications, Eng. Sci. Tech., Int. J. (2016), http://dx.doi.org/10.1016/j.jestch.2016.05.011

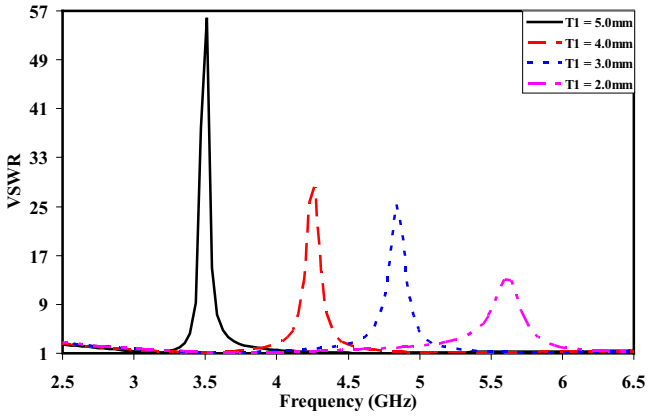

Fig. 4(a). Parametric variation of T_1 for WiMAX (3.3–3.8 GHz) band.

of T-shaped stub, wider shift of band-notch is observed from 3.35–3.85 GHz to 4.89–5.89 GHz which infers that length T_2 is alone capable of covering both WiMAX and WLAN bands with VSWR varying from 78.81 to 15.20 respectively. The length of T_2 from 3.0 mm to 11.0 mm is varied and shifting of band can be seen from higher to lower frequency side. The length T_2 is tuned to 11 mm with maximum VSWR of 55.81 to achieve intended notch band. The total length of the stub is given by $L_{\text{First Notch}} = T_1 + T_2$ and optimized values of T_1 and T_2 results in WiMAX band (3.25–3.82 GHz). During optimization of T_2, it has been observed that impedance bandwidth is maintained in the entire band (2.49–19.41 GHz) significantly.

3.3. Effect of slot length (W_4)

For the second notch as shown in Fig. 4(c), centered at 5.58 GHz, length of the second slot is calculated as $L_{\text{Second Notch}} = W_1 + 2(W_4 + L_1)$ mm. By varying W_4 from 2.75 mm to 3.25 mm, VSWR curve shifts from higher to lower frequency band. Also by optimizing $W_4 = 2.75$ mm desired WLAN band (4.83–5.99 GHz) is achieved. VSWR values at notch varies from 31.72 to 32.44. Impedance bandwidth in the entire band (2.49–19.41 GHz) is also maintained appreciably throughout optimization of W_4.

3.4. Effect of slot length (W_3)

For the third notch as shown in Fig. 4(d), centered at 7.47 GHz, length of the second slot is calculated as $L_{\text{Third Notch}} = W_2 + 2(W_3 + L_2)$ mm. By varying W_3 from 2.0 mm to 3.0 mm, VSWR curve shifts from higher to lower frequency band. By optimizing $W_3 = 3.0$ mm desired X-band (6.89–8.10 GHz) is achieved. VSWR

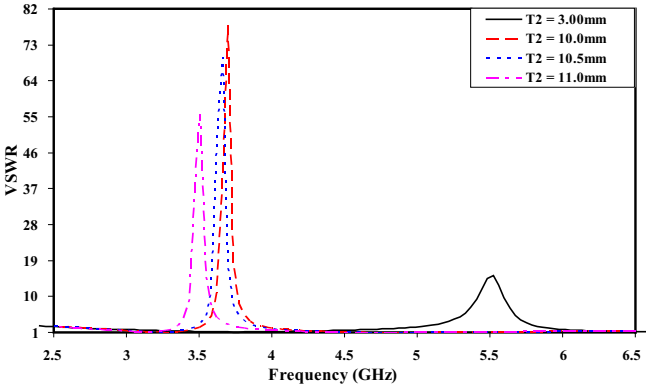

Fig. 4(b). Parametric variation of T_2 for WiMAX (3.3–3.8 GHz) band.

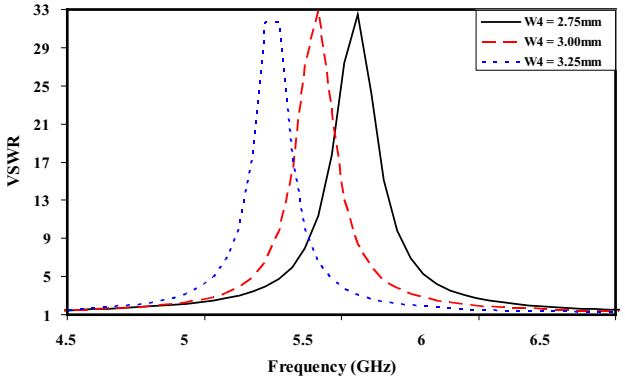

Fig. 4(c). Simulated parametric variation for WLAN (5.15–5.825 GHz).

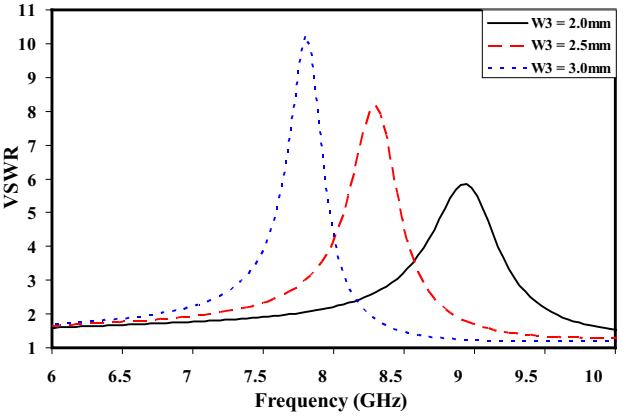

Fig. 4(d). Simulated parametric variation for X-band (7.1–7.9 GHz).

values at notch varies from 5.83 to 10.23. Impedance bandwidth in the entire band (2.49–19.41 GHz) is also maintained appreciably throughout optimization of W_3.

UWB devices did cause interference to the station when they were operated in close proximity and particularly within the main lobe of the antenna of the satellite receiving station. More UWB devices also caused more interference because of their aggregated effect. If UWB devices with output power spectral density of −41.3 dBm/MHz are to operate at the X-band, we should not allow such devices to go near to the X-band TV satellite receiver. If they are moved to 10 m away, the interference effect can be negligible. So, preferable a "No UWB Device" zone with radius at least 10 m should be declared surrounding the dish antenna of satellite receiver and hence the interference is mitigated. But in the latest technology 10 m radius is too large. Therefore, to avoid interference we introduced notch in X-band so that the UWB devices can be installed in close vicinity. So, the third notch (X-band: 7.25–7.75 GHz) is required.

3.5. Effect of stub width t_1, slot width t_2 and t_3

Table 1 represents simulated parametric variation of stub width t_1, slot width t_2 and t_3. Optimized values are given below.

The reason behind optimization analysis for three notch bands is due to the interferences of these narrow bands communication system with UWB systems should be avoided for better performance as well as increasing the level of power emission. However, the use of band stop filter requires more space to integrate, and it also increases the cost and complexity of the system. A better way

Please cite this article in press as: M. Sharma et al., Compact printed high rejection triple band-notch UWB antenna with multiple wireless applications, Eng. Sci. Tech., Int. J. (2016), http://dx.doi.org/10.1016/j.jestch.2016.05.011

Table 1
Parametric variation of notched-bandwidth by varying width of stub and slots (t_1, t_2, & t_3 as shown in Fig. 1c).

t_1 (mm)	BW (GHz)	t_2 (mm)	BW (GHz)	t_3 (mm)	BW (GHz)
0.25	0.62	0.25	0.613	0.25	0.720
0.50	0.53	0.50	0.688	0.50	0.813
0.75	0.48	0.75	0.930	0.75	1.182

to avoid interference is using UWB antenna with band notch characteristics.

4. Analysis of current distribution, input impedance and time domain analysis

In order to understand the phenomenon behind this triple band-stop performance, the simulated current distribution for the proposed antenna at the notch frequencies (3.56, 5.58 and 7.47 GHz) presented in Fig. 5.

As illustrated in Fig. 5(a) for the first notched-band current density is concentrated more at the inverted T-shaped stub (WiMAX), for the second notched-band current density distribution is concentrated at the inner and outer edge of the larger C-shaped slot (WLAN) as shown in Fig. 5(b) and Fig. 5(c) represents current density concentration at the smaller C-shaped slot (X-band). Furthermore, the strong current distributions around stub/slots at the notched frequency leads to near field radiation counteracted, due to which high energy is reflected back to the input port and the band-notched characteristics achieved. It is also can be noticed that in Fig. 5(a)–(c) there are very low mutually coupling at notch frequencies, which indicate that each rejected band can be controlled independently. In addition it is also observed that at entire frequency pass band except triple band-notch, the surface current is distributed uniformly over antenna.

It can be observed from Fig. 6(a), impedance bandwidth from 2.90 to 19.32 GHz. It is clear from Smith chart in Fig. 6(b) that all the three notch band for WiMAX (3.24–3.83 GHz), WLAN (4.86–5.99 GHz) and X-band (7.18–7.76 GHz) are rejected. For remaining UWB band the smith curve is well below VSWR = 2.0.

The simulated input signal and impulse response for the proposed antenna is shown in Fig. 7(a). Pulse distortion which is one of the characteristics of UWB signals is essentially determined by their wide bandwidth. To overcome minimize reflection loss and to avoid pulse distortion good impedance match has to be maintained throughout the operating band. The main reason between the signal distortion as shown in Fig. 7(a) is due to mismatch between source pulse and the antenna.

As a result, some frequency components cannot be transmitted effectively by the monopole, leading to the distortions of the received signal. Fig. 7(b) represents the group delay of proposed antenna without and with notch. Group delay is an important parameter for UWB and other communications since it can judge the distortion of transmitted pulses. For the perfect pulse transmission, the group delay should be closed to a constant within the entire band. It can be also concluded that the proposed antenna has perfect performance in this aspect, which makes it quite suitable for UWB as well as other high band wireless communication.

Table 2
Comparison of the proposed antenna with several existing designs.

Impedance bandwidth (GHz)	Notched bands	Bandwidth of notched bands	Maximum peak VSWR at center frequency	Maximum Gain (dBi)	Size (mm^2)
2.50–11.85 GHz	WiMAX WLAN X-band	3.20–3.90 GHz = 0.70 GHz 5.30–6.20 GHz = 0.90 GHz 7.00–8.20 GHz = 1.20 GHz	7.00 at 3.50 GHz 6.64 at 5.60 GHz 7.50 at 7.55 GHz	9.00	30 × 35 [21]
2.80–10.70 GHz	WiMAX WLAN X-band	3.10–3.80 GHz = 0.70 GHz 5.20 GHz-6.20 GHz = 1.00 GHz 7.10–8.10 GHz = 1.00 GHz	4.20 at 3.50 GHz 4.40 at 5.50 GHz 5.20 at 7.80 GHz	3.80	30 × 30 [30]
2.59–11.16 GHz	WiMAX WLAN X-band	3.29–3.61 GHz = 0.32 GHz 4.65–5.49 GHz = 0.84 GHz 7.30–8.41 GHz = 1.11 GHz	5.80 at 3.40 GHz 6.30 at 5.30 GHz 5.90 at 8.20 GHz	5.65	30 × 30 [34]
2.49–19.41 GHz	WiMAX WLAN X-band	3.17–3.89 GHz = 0.72 GHz 4.87–6.19 GHz = 1.32 GHz 7.23–7.86 GHz = 0.56 GHz	16.60 at 3.58 GHz 22.4 at 5.52 GHz 6.38 at 7.50 GHz	5.98	20 × 20 [*P]

* Proposed antenna.

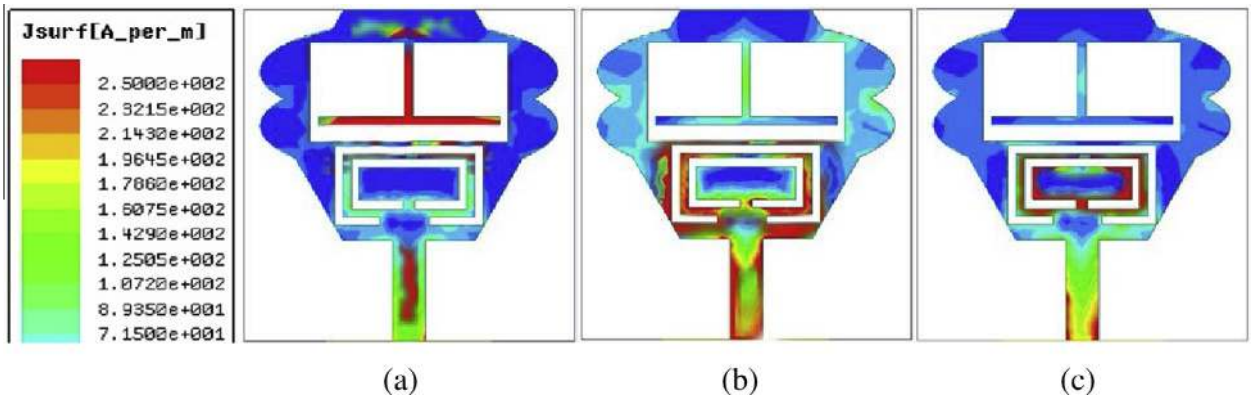

Fig. 5. Current density distribution (a) 3.56 GHz (b) 5.58 GHz (c) 7.47 GHz.

Please cite this article in press as: M. Sharma et al., Compact printed high rejection triple band-notch UWB antenna with multiple wireless applications, Eng. Sci. Tech., Int. J. (2016), http://dx.doi.org/10.1016/j.jestch.2016.05.011

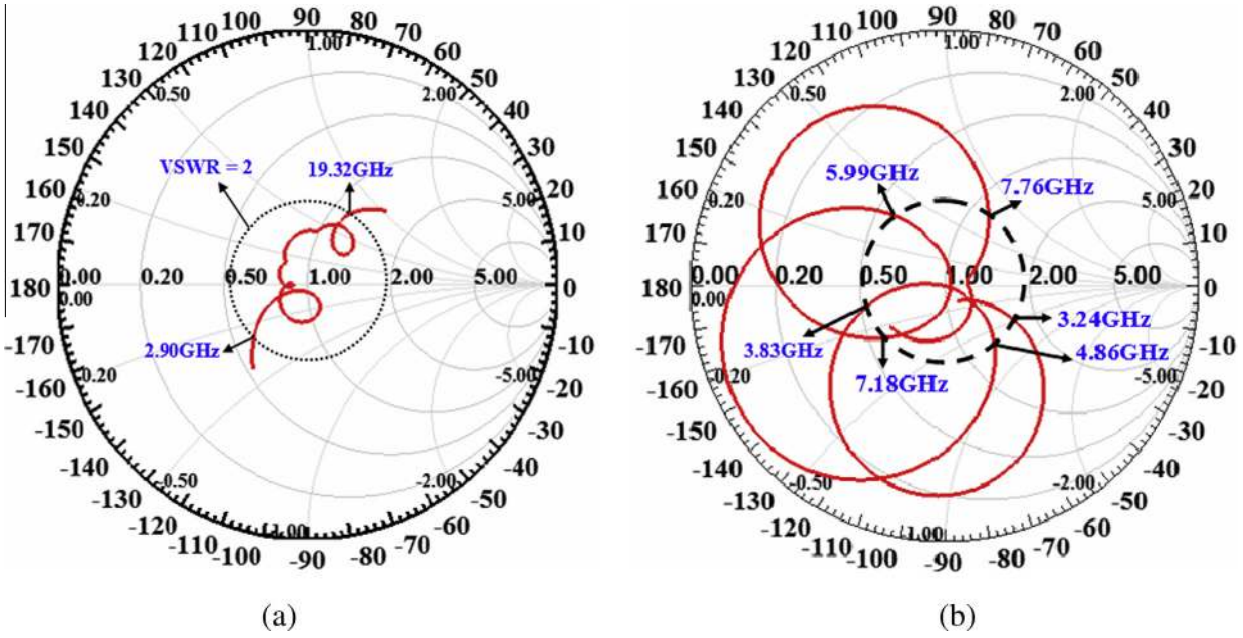

Fig. 6. Simulated input impedance on Smith chart (a) Proposed antenna bandwidth. (b) Triple band-notch UWB antenna.

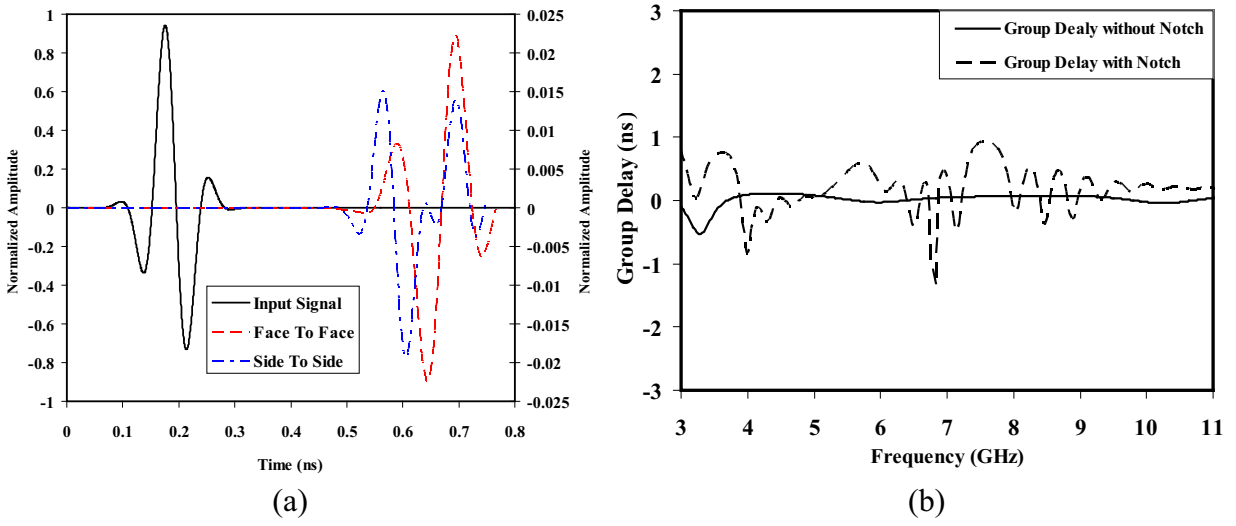

Fig. 7. (a) Simulated time domain analysis (input signal and impulse response). (b) Simulated group delay of without and with notch of proposed antenna.

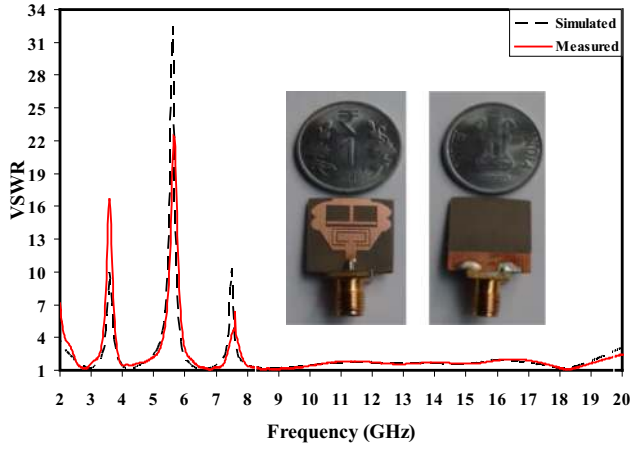

Fig. 8(a). Measured and simulated VSWR of the proposed antenna.

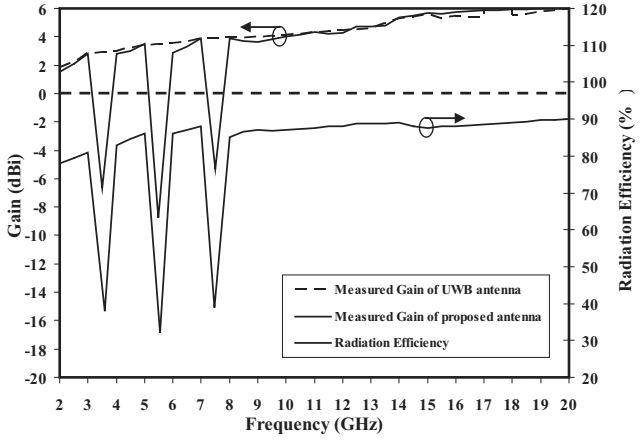

Fig. 8(b). Measured gain and simulated radiation efficiency of antenna.

Please cite this article in press as: M. Sharma et al., Compact printed high rejection triple band-notch UWB antenna with multiple wireless applications, Eng. Sci. Tech., Int. J. (2016), http://dx.doi.org/10.1016/j.jestch.2016.05.011

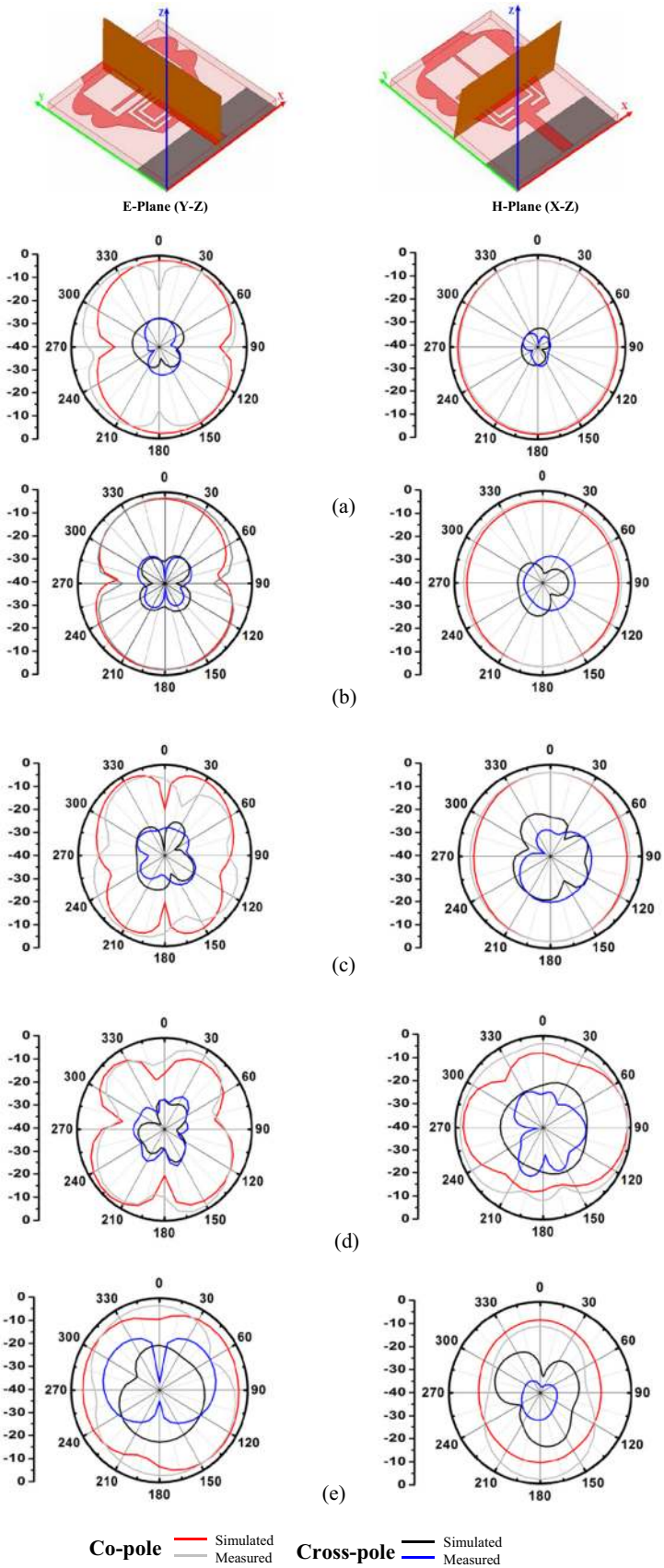

Fig. 9. Simulated & Measured radiation pattern of E and H-plane in dB at (a) 4.0 GHz (b) 6.5 GHz (c) 10.0 GHz (d) 15.0 GHz (e) 18.0 GHz.

Please cite this article in press as: M. Sharma et al., Compact printed high rejection triple band-notch UWB antenna with multiple wireless applications, Eng. Sci. Tech., Int. J. (2016), http://dx.doi.org/10.1016/j.jestch.2016.05.011

5. Experimental results

To demonstrate the above-discussed design strategy, an antenna prototype is fabricated. With comparison, both the measured and simulated VSWR characteristics of the proposed antenna are in good agreement within the entire band as depicted in Fig. 8 (a). The fabricated antenna has frequency band of 2.49 to over 19.41 GHz with three rejection bands around 3.17–3.89, 4.87–6.19 and 7.30–7.86 GHz. A discrepancy between the measured data and the simulated results exists, which could be due to the effect of the SMA port. By carefully performing the manufacturing and measurement process more accurate results can be obtained.

Measured gain of the proposed antenna and simple UWB-Ku band is shown in Fig. 8(b). A drop in peak gain is noted in notch band 6.62 at 3.60 GHz, 8.75 at 5.58 GHz and 5.32 at 7.60 GHz respectively. Effect of the three notches for WiMAX/WLAN and X-band are analyzed. At the three notched bands the gain falls down below 0 dBi which confirms that antenna does not radiate, whereas gain is almost matched in the remaining UWB, X and Ku bands without notched. The antenna gain varies from 2.08 to 5.98 dBi.

Simulated radiation efficiency is also shown in Fig. 8(b). Proposed antenna exhibits a good efficiency, being greater than 85% across the entire radiating band except in three notched bands. Furthermore, the simulated radiation efficiencies of the proposed triple band-notched antenna, at 3.58, 5.56 and 7.47 GHz are only 38%, 32% and 39% respectively.

The radiation of the fabricated UWB is presented in two principle planes (H-plane and E-plane). They are referred as E-plane (y–z plane) and H-plane (x–z plane). Fig. 9 shows the normalized simulated & measured radiation pattern in E-plane and H-plane at frequencies of 4.0, 6.5, 10.0, 15.0 & 18.0 GHz.

The measured radiation pattern at the pass band frequencies shows that the antenna is able to retain its omni-directional behavior in H-plane at lower frequencies while there is a little variation at higher frequencies due to cross-polarization. However, radiation pattern at higher frequencies deteriorates due to change in area of radiation.

6. Conclusion

In this paper, a compact urn-shape antenna is successfully presented and designed with the dimensions of $20 \times 20 \times 0.787$ mm^3. The antenna shows the good impedance matching characteristics within operating band from 2.49 to 19.41 GHz including three high rejection notch bands WiMAX, WLAN, and X-band downlink satellite system in UWB and multiple other wireless services as close range radar in X-band & satellite communication in Ku-band. Structural modification in the radiating patch increases the impedance bandwidth to 154.56% and achieved 55% size reduction. Proposed antenna is a good candidate for UWB and higher band communication applications.

Acknowledgement

The Authors are thankful to Krishna Ranjan Jha, Advance Microwave Antenna Testing Laboratory URL:delhi.gov.in/wps/wcm/connect/doit_gbpec/GBPEC/Home/List+of+Labs), G. B. Pant Engineering College, Delhi for providing Antenna Measurement Facility.

References

[1] M.M.S. Taheri, H.R. Hassani, S.M.A. Nezhad, UWB printed slot antenna with bluetooth and dual notch bands, IEEE Antennas Wirel. Propag. Lett. 10 (2011) 255–258.
[2] W. Jiang, W. Che, A novel UWB antenna with dual notched bands for WiMAX and WLAN applications, IEEE Antennas Wirel. Propag. Lett. 11 (2012) 293–296.
[3] M. Ojaroudi, N. Ojaroudi, N. Ghadimi, Dual band-notched small monopole antenna with novel coupled inverted U-ring strip and novel fork-shaped slit for UWB applications, IEEE Antennas Wirel. Propag. Lett. 12 (2013) 182–185.
[4] N. Ojaroudi, M. Ojaroudi, Novel design of dual band-notched monopole antenna with bandwidth enhancement for UWB applications, IEEE Antennas Wirel. Propag. Lett. 12 (2013) 698–701.
[5] S.M. Abbas, Y. Ranga, A.K. Verma, K.P. Esselle, A simple ultra wideband monopole antenna with high band rejection and wide radiation patterns, IEEE Trans. Antennas Propag. 62 (9) (2014) 4816–4820.
[6] R. Chandel, A.K. Gautam, B.K. Kanaujia, Microstrip-line fed beak-shaped monopole-like slot UWB antenna with enhanced band width, Microwave Opt. Technol. Lett. 56 (11) (2014) 2624–2628.
[7] A. Foudazi, H.R. Hassani, S. Mohammad, A. Nehzad, Small UWB planar monopole antenna with added GPS/GSM/WLAN bands, IEEE Trans. Antennas Propag. 60 (6) (2012) 2987–2992.
[8] S. Mohammad, A. Nehzad, H.R. Hassani, A. Foudazi, A Dual-band WLAN/UWB printed wide slot antenna for MIMO/diversity applications, Microwave Opt. Technol. Lett. 5 (6) (2013) 461–465.
[9] C.M. Dikmen, S. Cimen, G. Cakir, Planar octagonal-shaped UWB antenna with reduced radar cross section, IEEE Trans. Antennas Propag. 62 (6) (2014) 2945–2953.
[10] D. Unnikrishnan, D. Kaddour, S. Tedjini, E. Bihar, M. Saddaoui, CPW-fed inkjet printed UWB antenna on ABS-PC for integration in molded interconnect devices technology, IEEE Antennas Wirel. Propag. Lett. 14 (2015) 1125–1128.
[11] A.T. Mobashsher, A. Abbosh, Utilizing symmetry of planar ultrawideband antennas for size reduction and enhanced performance, IEEE Antennas Propag. Mag. 57 (2) (2015) 153–166.
[12] R. Natarajan, J.V. George, M. Kanagasabai, A.K. Shrivastava, A compact antipodal vivaldi antenna for UWB applications, IEEE Antennas Wirel. Propag. Lett. 14 (2015) 1557–1560.
[13] F.M. Alnahwi, K.M. Abdulhasan, N.E. Islam, An ultrawideband to dual-band switchable antenna design for wireless communication applications, IEEE Antennas Propag. Mag. 57 (14) (2015) 1685–1688.
[14] M.N. Moghadasi, R.A. Sadeghzadeh, T. Sedghi, T. Aribi, B.S. Virdee, UWB CPW-fed Fractal Patch antenna with Band-notched function employing folded T-shaped element, IEEE Antennas Wirel. Propag. Lett. 12 (2013) 504–507.
[15] P. Beigi, J. Nourinia, B. Mohammadi, A. Valizade, Bandwidth enhancement of small square monopole antenna with dual band notch characteristics using U-shaped slot and butterfly shape parasitic element on backplane for UWB applications, ACES 30 (1) (2015) 78–85.
[16] W.S. Yeoh, W.S.T. Rowe, An UWB conical monopole antenna for multiservice wireless applications, IEEE Antennas Wirel. Propag. Lett. 14 (2015) 1085–1088.
[17] A. Wu, B. Guan, A compact CPW-fed UWB antenna with dual band-notched characteristics, IEEE Antennas Wirel. Propag. Lett. 12 (2013) 151–154.
[18] A.K. Gautam, S. Yadav, B.K. Kanaujia, A CPW-fed compact UWB microstrip antenna, IEEE Antennas Wirel. Propag. Lett. 12 (2013) 151–154.
[19] A.K. Verma, Y.K. Awasthi, H. Singh, Equivalent isotropic relative permittivity of microstrip on multilayer anisotropic substrate, Int. J. Electron. 96 (8) (2009) 865–875.
[20] F.B. Zarrabi, Z. Mansouri, N.P. Gandji, H. Kuhestani, Triple-notch UWB monopole antenna with fractal Koch and T-shaped stub, Int. J. Electron. Commun. 70 (2016) 64–69.
[21] G. Srivastava, S. Dwari, B.K. Kanaujia, A compact triple band notch circular ring antenna for UWB applications, Microwave Opt. Technol. Lett. 57 (3) (2015) 668–672.
[22] M.K. Khandelwal, B.K. Kanaujia, S. Dwari, S. Kumar, A.K. Gautam, Triple band circularly polarized compact microstrip antenna with defected ground structure for wireless applications, Int. J. Microwave Technol. (2015) 1–11.
[23] N. Ojaroudi, M. Ojaroudi, Dual band-notched monopole antenna with multi-resonance characteristic for UWB wireless communications, Prog. Electromagn. Res. Lett. 40 (2013) 187–199.
[24] D. Zhou, S. Gao, F. Zhu, R.A.A. Alhameed, J.D. Xu, A simple and compact planar ultrawideband antenna with single or dual band-notched characteristics, Prog. Electromagn. Res. 123 (2012) 47–65.
[25] C.Y. Liu, T. Jiang, Y.S. Li, A compact wide slot antenna with dual band-notch characteristic for ultra wideband applications, J. Microwaves Optoelectron. Electromagn. Appl. 10 (1) (2011) 55–64.
[26] M.K. Khandelwal, B.K. Kanaujia, S. Dwari, S. Kumar, Analysis and design of wide band microstrip-line-feed antenna with defected ground structure for Ku band applications, Int. J. Electron. Commun. (2014) 951–957.
[27] G. Li, H. Zhai, T. Li, X. Ma, C. Liang, Design of a compact UWB antenna integrated with GSM/WCDMA/WLAN bands, Prog. Electromagn. Res. 136 (2013) 409–419.
[28] A. Nouri, G.R. Dadaszadeh, A compact UWB band-notched printed monopole antenna with defected ground structure, IEEE Antennas Wirel. Propag. Lett. 10 (2011) 1178–1182.
[29] M. Moosazadeh, A.M. Abbosh, Z. Esmati, Design of compact planar ultrawideband antenna with dual- notched bands using slotted square patch and pi-shaped conductor-backed plane, IET Microwaves, Antennas Propag. 6 (3) (2012) 290–294.
[30] S. Tomar, A. Kumar, Design of a triple band-notched UWB planar monopole antenna, J. Microwaves Optoelectron. Electromagn. Appl. 14 (2) (2015) 184–196.
[31] S.K. Venkata, M. Rana, P.S. Bakariya, S. Dwari, M. Sarkar, Planar UWB monopole antenna with Tri-notch band characteristics, Prog. Electromagn. Res. C 46 (2014) 163–170.

Please cite this article in press as: M. Sharma et al., Compact printed high rejection triple band-notch UWB antenna with multiple wireless applications, Eng. Sci. Tech., Int. J. (2016), http://dx.doi.org/10.1016/j.jestch.2016.05.011

[32] D. Zhao, C. Yang, M. Zhu, Z. Chen, Design of WLAN/LTE/UWB antenna with improved pattern uniformity ground-cooperative radiating structure, IEEE Trans. Antennas Propag. 64 (2016) 271–276.

[33] M.C. Tang, T. Shi, W. Ziolkowski, Planar ultrawideband antennas with improved realized gain performance, IEEE Trans. Antennas Propag. 64 (1) (2016) 61–69.

[34] S. Das, D. Mitra, S.R.B. Chaudhri, Design of UWB planar monopole antennas with etched spiral slot on the patch for multiple band-notched characteristics, Int. J. Microwave Sci. Technol. (2015) 1–9.

[35] R.V.S.R. Krishna, R. Kumar, A slotted UWB monopole antenna with single port and double ports for dual polarization, Eng. Sci. Technol. Int. J. 19 (2016) 470–484.

Please cite this article in press as: M. Sharma et al., Compact printed high rejection triple band-notch UWB antenna with multiple wireless applications, Eng. Sci. Tech., Int. J. (2016), http://dx.doi.org/10.1016/j.jestch.2016.05.011